

Characteristics of graviton-induced bremsstrahlung

Erik Dvergsnes, Per Osland, Nurcan Öztürk

Department of Physics, University of Bergen,
Allégaten 55, N-5007 Bergen, Norway

Abstract

We discuss Bremsstrahlung induced by graviton exchange in proton-proton interactions at hadronic colliders, resulting from $gg \rightarrow G \rightarrow \mu^+\mu^-\gamma$. Both the ADD and RS scenarios are discussed. Due to the coupling of the graviton to two photons, the cross section has a new kinematical singularity for hard photons. Thus, graviton-induced Bremsstrahlung tends to yield more hard photons than QED-based Bremsstrahlung. As compared with the corresponding two-body final state, $\mu^+\mu^-$, the cross section is, for realistic cuts, smaller by a factor ~ 0.02 . At the LHC, and with a string scale of a few TeV (ADD scenario), or a graviton mass of a few TeV (RS scenario), a few events of high invariant mass are expected per year.

1 Introduction

The idea of additional compact dimensions and strings at the TeV scale, proposed by Antoniadis [1] for solving the hierarchy problem, together with the idea that Standard-Model (SM) fields live on branes in a higher-dimensional space [2] have led to the even more radical speculations that extra dimensions might be macroscopic, with SM fields confined to the familiar four-dimensional world (brane) [3, 4]. The models which allow for gravity effects at the TeV scale can be grouped into two kinds, those of factorizable geometry, where the extra dimensions are macroscopic [3] (“ADD scenario”), and those of non-factorizable (warped) geometry, with only one extra dimension separating “our” brane from a hidden brane [4] (“RS scenario”).

In both these scenarios, the propagation of gravitons in the extra dimensions leads to gravitons which from the four-dimensional point of view are massive. In the ADD scenario, these Kaluza–Klein (KK) gravitons have masses starting at values of the order of milli-eV, and there is practically a continuum of them, up to some cut-off M_S (string scale) of the order of TeV, whereas in the RS scenario they are widely separated resonances at the TeV scale. In both cases, they have a universal coupling to matter and photons via the energy-momentum tensor.

These recent speculations have led to several studies [5–12] of various experimental signals induced by graviton production and exchange. The new scenarios allow for the emission of massive gravitons [5, 6, 7], which would lead to events with missing energy (or transverse momentum), as well as effects due to the exchange of virtual gravitons (instead of photons or Z^0 s) [5, 7, 8, 11]. These include the production of dileptons and diphotons in electron-positron collisions, as well as gluon-gluon and quark-antiquark-induced processes at the Tevatron and LHC.

In fact, several searches at LEP and the Tevatron have given direct bounds on M_S [13] of the order of a TeV, while astrophysical arguments [14] can rule out M_S up to a scale of around 80 TeV¹. Of course, a direct experimental search would be most worthwhile. The above studies all focus on two-particle final states, which are expected to be dominant, and therefore lead to the most stringent bounds on the existence of massive gravitons.

Here, we shall investigate Bremsstrahlung induced by graviton exchange. While this cross section is further reduced by $\mathcal{O}(\alpha/\pi)$, so is the background. It has some characteristic features resulting from the exchange of a spin-2 particle and from the direct graviton-photon coupling, that we would like to point out. These features may be useful in discriminating any signal against the background.

Specifically, we shall consider the process

$$pp \rightarrow \mu^+ \mu^- \gamma + X, \tag{1}$$

which may get a contribution due to graviton exchange, and which for energetic muons and photons should experimentally be a very clean signal.

¹This value applies to the simplest ADD scenario, for $n = 2$ extra dimensions.

We shall here focus on the gluon-gluon initiated sub-process

$$gg \rightarrow G \rightarrow \mu^+ \mu^- \gamma. \quad (2)$$

There is also an annihilation process:

$$q\bar{q} \rightarrow G \rightarrow \mu^+ \mu^- \gamma, \quad (3)$$

which will interfere with the Drell–Yan background, but this is suppressed by a smaller convolution integral for moderate values of the invariant mass. At higher invariant masses, there is also a significant contribution from quark-antiquark annihilation, as will be discussed in detail elsewhere [15].

Since this final state is very distinct, and since the Drell–Yan (or QED) background is well understood, the process (1) may offer some hope for observing a signal or improving on the exclusion bounds.

2 Two-body final states

The process of interest, Eq. (1), is related to the two-body final state

$$pp \rightarrow \mu^+ \mu^- + X, \quad (4)$$

which may proceed via gluon fusion and an intermediate graviton,

$$gg \rightarrow G \rightarrow \mu^+ \mu^-. \quad (5)$$

For massless muons, the cross section for a single graviton exchange is²

$$\hat{\sigma}_{gg \rightarrow \mu^+ \mu^-}^{(G)}(\hat{s}) = \frac{\kappa^4}{10240\pi} \frac{\hat{s}^3}{(\hat{s} - m_G^2)^2 + (m_G \Gamma_G)^2}, \quad (6)$$

with $\hat{s} = (k_1 + k_2)^2$ the two-gluon invariant mass squared. Furthermore, m_G and Γ_G are the mass and width of the graviton, and κ is the graviton coupling, to be defined below. The angular distribution is given by $1 - \cos^4 \theta$, where θ is the c.m. scattering angle.

With ξ_1 and ξ_2 the fractional momenta of the two gluons, $k_1 = \xi_1 P_1$, $k_2 = \xi_2 P_2$, and P_1 and P_2 the proton momenta, $(P_1 + P_2)^2 = s$, we have $\hat{s} \simeq \xi_1 \xi_2 s$.

For the over-all process (4) we thus find

$$\sigma_{gg \rightarrow \mu^+ \mu^-}^{(G)} = \int_0^1 d\xi_1 \int_0^1 d\xi_2 f_g(\xi_1) f_g(\xi_2) \delta\left(\xi_1 \xi_2 - \frac{\hat{s}}{s}\right) \hat{\sigma}_{gg \rightarrow \mu^+ \mu^-}^{(G)}(\hat{s}) = I_{gg}(\hat{s}) \hat{\sigma}_{gg \rightarrow \mu^+ \mu^-}^{(G)}(\hat{s}), \quad (7)$$

²This result is in agreement with [12].

with

$$I_{gg}(\hat{s}) = \int_{-Y}^Y dy f_g \left(\sqrt{\frac{\hat{s}}{s}} e^y \right) f_g \left(\sqrt{\frac{\hat{s}}{s}} e^{-y} \right), \quad Y = \frac{1}{2} \log \frac{s}{\hat{s}}, \quad (8)$$

the relevant convolution integral over the gluon distribution functions. For the ADD scenario, it will be more convenient to compare with the differential cross section:

$$\begin{aligned} \frac{d\sigma_{gg \rightarrow \mu^+ \mu^-}^{(G)}}{d\hat{s}} &= \int_0^1 d\xi_1 \int_0^1 d\xi_2 f_g(\xi_1) f_g(\xi_2) \frac{d\hat{\sigma}_{gg \rightarrow \mu^+ \mu^-}^{(G)}}{d\hat{s}} \\ &= \int_0^1 d\xi_1 \int_0^1 d\xi_2 f_g(\xi_1) f_g(\xi_2) \delta(\xi_1 \xi_2 s - \hat{s}) \hat{\sigma}_{gg \rightarrow \mu^+ \mu^-}^{(G)}(\hat{s}) \\ &= \frac{1}{s} I_{gg}(\hat{s}) \hat{\sigma}_{gg \rightarrow \mu^+ \mu^-}^{(G)}(\hat{s}). \end{aligned} \quad (9)$$

3 Graviton-induced Bremsstrahlung

The Bremsstrahlung process (2) can proceed via the four Feynman diagrams of Fig. 1, the basic couplings for which are given by Han et al. [7] (see also Giudice et al. [5]).

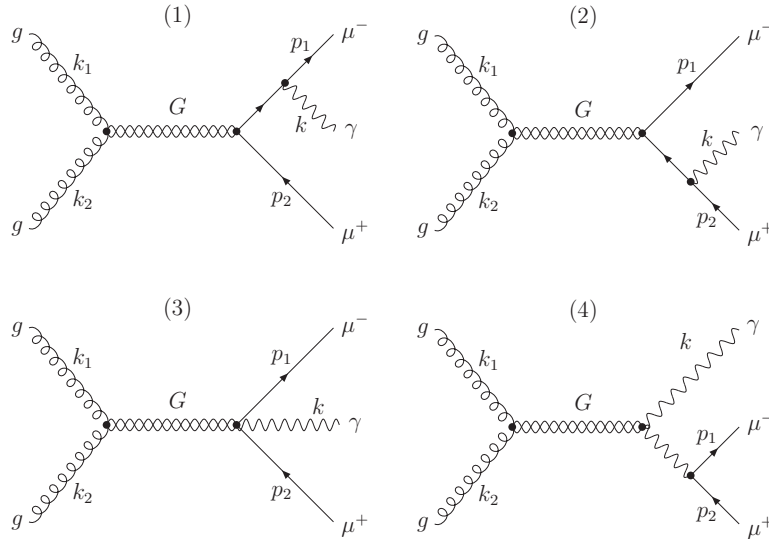


Figure 1: Feynman diagrams for $gg \rightarrow G \rightarrow \mu^+ \mu^- \gamma$.

The evaluation of the cross section is straightforward. We choose the (unitary) gauge ($\xi^{-1} = 0$ in the notation of [7]), whereby the scalar field decouples. The resulting cross

section has in the two-gluon c.m. frame the form (again for a single graviton exchange):

$$\frac{4\pi}{d(\cos\theta)d\chi} \frac{d^4\hat{\sigma}_{gg\rightarrow\mu^+\mu^-\gamma}^{(G)}}{dx_1dx_2} = \frac{\alpha\kappa^4}{2560\pi^2} \frac{\hat{s}^3}{(\hat{s} - m_G^2)^2 + (m_G\Gamma_G)^2} \frac{Z(x_1, x_2, \cos\theta, \chi)}{(1 - 2x_1)(1 - 2x_2)(1 - 2x_3)}, \quad (10)$$

where α is the fine-structure constant and x_1 , x_2 and x_3 denote the fractional energies of the muons and the photon in the c.m. frame,

$$x_1 = E_1/\sqrt{\hat{s}}, \quad x_2 = E_2/\sqrt{\hat{s}}, \quad x_3 = \omega/\sqrt{\hat{s}}, \quad 0 \leq x_i \leq \frac{1}{2}, \quad (11)$$

with $x_1 + x_2 + x_3 = 1$, whereas θ and χ give the orientation of the event w.r.t. the gluon momenta, and

$$\hat{s} \equiv (k_1 + k_2)^2 = (p_1 + p_2 + k)^2. \quad (12)$$

The denominator in (10) exhibits the familiar singularities in the infrared and collinear limits, $s_1 \equiv (p_1 + k)^2 = \hat{s}(1 - 2x_2) \rightarrow 0$, $s_2 \equiv (p_2 + k)^2 = \hat{s}(1 - 2x_1) \rightarrow 0$, as well as a collinear singularity at $s_3 \equiv (p_1 + p_2)^2 = \hat{s}(1 - 2x_3) \rightarrow 0$ due to the fourth Feynman diagram.

Since the underlying mechanism is the exchange of a spin-two object, the quantity Z is of fourth order in the invariants. It is straight-forward to verify that it is gauge invariant with respect to the gluons, as well as to the photon (actually, diagram 4 is by itself gauge invariant). But the expression is quite lengthy, so we shall not write it out here.

The angular distribution of the non-radiative cross section (6) is given by a fourth-order polynomial in $\cos\theta$. Here, just like in gluon Bremsstrahlung (see, e.g., [16]), there is an accompanying dependence on the azimuthal angle χ , but now up to fourth order in $\cos\chi$, or, equivalently, up to $\cos 4\chi$.

After averaging and summing over gluon, muon and photon polarizations, and integrating over event orientations w.r.t. the gluon momentum, we find

$$\frac{d^2\hat{\sigma}_{gg\rightarrow\mu^+\mu^-\gamma}^{(G)}}{dx_1dx_2} = \frac{\alpha\kappa^4}{2560\pi^2} \frac{\hat{s}^3}{(\hat{s} - m_G^2)^2 + (m_G\Gamma_G)^2} \frac{Z(x_1, x_2)}{(1 - 2x_1)(1 - 2x_2)(1 - 2x_3)}, \quad (13)$$

with

$$\begin{aligned} Z(x_1, x_2) &= 2(x_1^2 + x_2^2)[16x_1x_2 - 6(x_1 + x_2) + 3] \\ &= 2(x_1^2 + x_2^2)[1 - 2x_3 + 4x_3^2 - 4(x_1 - x_2)^2]. \end{aligned} \quad (14)$$

describing the event-shape distribution.

For the over-all process (1) we thus find from Eq. (7)

$$\frac{d^2\sigma_{gg\rightarrow\mu^+\mu^-\gamma}^{(G)}}{dx_1dx_2} = I_{gg}(\hat{s}) \frac{d^2\hat{\sigma}_{gg\rightarrow\mu^+\mu^-\gamma}^{(G)}}{dx_1dx_2}, \quad (15)$$

with the relevant convolution integral over the gluon distribution functions given by Eq. (8). Using Eq. (13), we get

$$\frac{1}{\sigma_{gg \rightarrow \mu^+ \mu^-}^{(G)}} \frac{d^2 \sigma_{gg \rightarrow \mu^+ \mu^- \gamma}^{(G)}}{dx_1 dx_2} = \frac{4\alpha}{\pi} \frac{Z(x_1, x_2)}{(1-2x_1)(1-2x_2)(1-2x_3)}, \quad (16)$$

with $\sigma_{gg \rightarrow \mu^+ \mu^-}^{(G)}$ given by Eqs. (6) and (7).

4 Bremsstrahlung in the ADD scenario

In the ADD scenario [3], the coupling of each KK mode to matter is Planck-scale suppressed. However, since the states are very closely spaced, with [7]

$$m_G^2 = \frac{4\pi^2 \bar{n}_{\text{KK}}^2}{R^2}, \quad (17)$$

and $R/2\pi$ the compactification radii, the coherent summation over the many modes leads to effective couplings with strength $1/M_S$.

Explicitly, in this scenario, the graviton coupling is in the $(4+n)$ -dimensional theory given by [7]

$$\hat{g}_{MN} = \hat{\eta}_{MN} + \hat{\kappa} \hat{h}_{MN}, \quad \hat{\kappa}^2 = 16\pi G_N^{(4+n)}, \quad (18)$$

where $G_N^{(4+n)}$ is Newton's constant in $4+n$ dimensions. In 4 dimensions the coupling can be written as

$$\kappa^2 = V_n^{-1} \hat{\kappa}^2 = 16\pi V_n^{-1} G_N^{(4+n)} = 16\pi G_N, \quad (19)$$

with V_n the volume of the n -dimensional compactified space ($V_n = R^n$ for a torus T^n) and G_N the 4-dimensional Newton constant.

Summing coherently over all KK modes in a tower, the graviton propagator gets replaced [7]:

$$\frac{i}{\hat{s} - m_G^2} \rightarrow D(\hat{s}) = \frac{8\pi}{\kappa^2} C_4, \quad (20)$$

with

$$C_4 \simeq \begin{cases} -iM_S^{-4} \log(M_S^2/\hat{s}), & n = 2, \\ -2iM_S^{-4}/(n-2), & n > 2, \end{cases} \quad (21)$$

for n extra dimensions, and $M_S \gg \sqrt{\hat{s}}$ the string scale which is introduced as an UV cut-off.

The Bremsstrahlung cross section can thus be expressed as

$$\frac{d^3\sigma_{gg\rightarrow\mu^+\mu^-\gamma}^{(G)}}{d\hat{s}dx_1dx_2} = \frac{\alpha\kappa^4}{2560\pi^2} \frac{\hat{s}^3}{s} |D(\hat{s})|^2 \frac{Z(x_1, x_2)}{(1-2x_1)(1-2x_2)(1-2x_3)} I_{gg}(\hat{s}). \quad (22)$$

For a given value of \hat{s} (characterizing the final state) the cross section depends on three model parameters: n , M_S and R , which are related as follows [7]:

$$\kappa^2 R^n = 8\pi(4\pi)^{n/2}\Gamma(n/2)M_S^{-(n+2)}. \quad (23)$$

Relative to the two-body cross section, the Bremsstrahlung cross section is however *independent of the ADD model parameters*:

$$\left[\frac{d\sigma_{gg\rightarrow\mu^+\mu^-}^{(G)}}{d\hat{s}} \right]^{-1} \frac{d^3\sigma_{gg\rightarrow\mu^+\mu^-\gamma}^{(G)}}{d\hat{s}dx_1dx_2} = \frac{4\alpha}{\pi} \frac{Z(x_1, x_2)}{(1-2x_1)(1-2x_2)(1-2x_3)}, \quad (24)$$

where $\sigma_{gg\rightarrow\mu^+\mu^-}^{(G)}$ refers to the gluon-gluon-induced two-muon cross section³

$$\frac{d\sigma_{gg\rightarrow\mu^+\mu^-}^{(G)}}{d\hat{s}} = \frac{\pi}{160} \frac{\hat{s}^3}{s} |C_4|^2 I_{gg}(\hat{s}). \quad (25)$$

5 Bremsstrahlung in the Randall–Sundrum model

In the Randall–Sundrum model [4], the graviton masses are given by [10]

$$(m_G)_n = kx_n e^{-kr_c\pi}, \quad (26)$$

where x_n are roots of the Bessel function of order 1, k is of the order of the (four-dimensional) Planck scale and r_c the compactification radius of the extra dimension⁴.

The gravitational coupling is for the lightest KK-graviton given by⁵ [10, 12]

$$\kappa m_G = \sqrt{2}x_1 \frac{k}{\overline{M}_{\text{Pl}}}, \quad \overline{M}_{\text{Pl}} = \frac{M_{\text{Pl}}}{\sqrt{8\pi}} \simeq 2.4 \times 10^{18} \text{ GeV}, \quad (27)$$

where $x_1 = 3.83171$ is the first zero of the Bessel function, $J_1(x_1) = 0$.

In the Randall–Sundrum model, the gravitons are thus rather massive and widely separated in mass. For small values of $k/\overline{M}_{\text{Pl}}$, it is an excellent approximation to integrate (6) and (15) over \hat{s} in the narrow-width approximation,

$$\int d\hat{s} \frac{1}{(\hat{s} - m_G^2)^2 + (m_G\Gamma_G)^2} f(\hat{s}) \simeq \frac{\pi}{m_G\Gamma_G} f(m_G^2), \quad (28)$$

³This result is consistent with that of [8].

⁴To solve the hierarchy problem, $kr_c \sim 12$ is required.

⁵For simplicity we will only consider the first resonance, and let m_G refer to its mass.

where [7, 17]

$$\Gamma_G \equiv \frac{\gamma_G}{20\pi} m_G^3 \kappa^2, \quad (29)$$

with

$$\gamma_G = 1 + \chi_\gamma + \chi_Z + \chi_W + \chi_\ell + \chi_q + \chi_H, \quad (30)$$

the total graviton width in units of the two-gluon width. Neglecting mass effects, we have [7, 17]

$$\chi_\gamma = \frac{1}{8}, \quad \chi_Z = \frac{13}{96}, \quad \chi_W = \frac{13}{48}, \quad \chi_\ell = \frac{N_\ell}{16}, \quad \chi_q = \frac{N_c N_q}{16}, \quad \chi_H = \frac{1}{48}. \quad (31)$$

Here, $N_\ell = 6$ is the number of leptons, and $N_c N_q = 18$ is the number of quarks weighted with color factors.

In the narrow-width approximation, the integrated cross section (15) becomes

$$\int d\hat{s} \frac{d^2 \sigma_{gg \rightarrow \mu^+ \mu^- \gamma}^{(G)}}{dx_1 dx_2} = \frac{\alpha}{128} \frac{(\kappa m_G)^2}{\gamma_G} I_{gg}(m_G^2) \frac{Z(x_1, x_2)}{(1-2x_1)(1-2x_2)(1-2x_3)}. \quad (32)$$

6 Drell–Yan (QED) background

The same final state can also be produced by

$$q\bar{q} \rightarrow \gamma, Z^0 \rightarrow \mu^+ \mu^- \gamma. \quad (33)$$

Photon exchange dominates over Z^0 exchange, and gives an elementary $q\bar{q} \rightarrow \gamma \rightarrow \mu^+ \mu^- \gamma$ cross section⁶

$$\frac{d^2 \hat{\sigma}_{q\bar{q} \rightarrow \mu^+ \mu^- \gamma}^{(\gamma)}}{dx_1 dx_2} = \frac{32}{9} \frac{\alpha^3}{\hat{s}} \frac{x_1^2 + x_2^2}{(1-2x_1)(1-2x_2)} \quad (34)$$

(divided by the quark charge squared, Q_q^2). For proton-proton collisions, we get

$$\frac{d^2 \sigma_{q\bar{q} \rightarrow \mu^+ \mu^- \gamma}^{(\gamma)}}{dx_1 dx_2} = I_{q\bar{q}}(\hat{s}) \frac{d^2 \hat{\sigma}_{q\bar{q} \rightarrow \mu^+ \mu^- \gamma}^{(\gamma)}}{dx_1 dx_2}, \quad (35)$$

with

$$I_{q\bar{q}}(\hat{s}) = 2 \sum_q Q_q^2 \int_{-Y}^Y dy f_q \left(\sqrt{\frac{\hat{s}}{s}} e^y \right) f_{\bar{q}} \left(\sqrt{\frac{\hat{s}}{s}} e^{-y} \right) \quad (36)$$

⁶We neglect Bremsstrahlung from initial quarks, since this contribution can be substantially reduced by suitable cuts.

the appropriate quark-antiquark convolution integral for the LHC (the factor of two accounts for the fact that either beam can provide the quark or the antiquark). In the ADD case we will use Eq. (9), but now with the convolution integral from Eq. (36), to express the differential cross section for the QED background as

$$\frac{d^3\sigma_{q\bar{q}\rightarrow\mu^+\mu^-\gamma}^{(\gamma)}}{d\hat{s}dx_1dx_2} = \frac{1}{s} I_{q\bar{q}}(\hat{s}) \frac{d^2\hat{\sigma}_{q\bar{q}\rightarrow\mu^+\mu^-\gamma}^{(\gamma)}}{dx_1dx_2}. \quad (37)$$

In the RS scenario, the signal to background ratio will depend critically on the experimental resolution in \hat{s} , which we shall express in terms of

$$\delta_{\hat{s}} \equiv \frac{\Delta\hat{s}}{\hat{s}} = \frac{\Delta(p_1 + p_2 + k)^2}{\hat{s}}. \quad (38)$$

It is also useful to define dimensionless cross sections, integrated over event shapes, subject to y -cuts:

$$\tilde{\sigma}_{gg\rightarrow\mu^+\mu^-\gamma}^{(G)} = \iint_{s_i > y\hat{s}} dx_1 dx_2 \frac{Z(x_1, x_2)}{(1-2x_1)(1-2x_2)(1-2x_3)}, \quad (39)$$

$$\tilde{\sigma}_{q\bar{q}\rightarrow\mu^+\mu^-\gamma}^{(\gamma)} = \iint_{s_i > y\hat{s}} dx_1 dx_2 \frac{2(x_1^2 + x_2^2)}{(1-2x_1)(1-2x_2)}. \quad (40)$$

The y -cuts will remove IR soft and collinear events where the photon has little energy, or its direction is close to that of a muon. A milder y -cut, y_3 , will remove events where the two muons are close. These integrated cross sections will play a crucial role when we compare signal and background.

7 Event characteristics

It is interesting to compare the energy distribution for spin-two graviton exchange with the corresponding one resulting from the exchange of a spin-one object, like the photon or a Z^0 . In Fig. 2 we show $Z(x_1, x_2)/[2(1-2x_3)(x_1^2 + x_2^2)]$, which is the ratio of the integrands in Eqs. (39) and (40). (The normalization is chosen such that the ratio is 1 in the IR limit, $x_3 \rightarrow 0$, or $x_1 \simeq x_2 \rightarrow \frac{1}{2}$.)

The “wall” at $x_3 \rightarrow \frac{1}{2}$ is due to the collinear singularity that arises from the fourth diagram (see Fig. 1). Of course, when finite-mass effects are taken into account, the cross section is finite in this limit [15]. Integrating over some slice in x_3 along this “wall”, the cross section gets enhanced by a factor $\log(\hat{s}/4m_f^2)$, with m_f the muon mass. This partly compensates for the factor α/π .

Concerning the angular distributions, we note that the photon originating from the two-gluon initial state leads to no forward-backward asymmetry, as is the case for the two-body final states [5, 8]. On the other hand, with quark-antiquark initial states, there

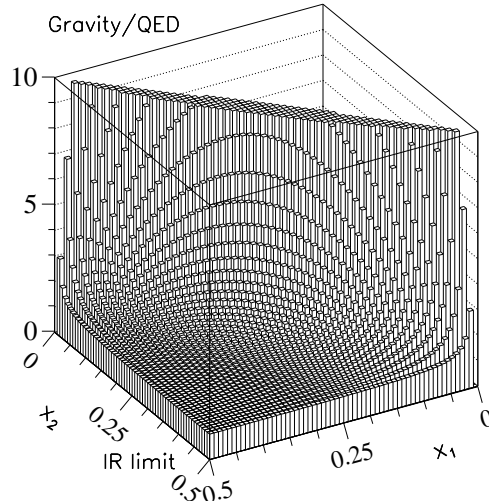


Figure 2: Ratio of graviton-induced to QED cross section, *vs.* fractional muon energies x_1 and x_2 . The ratio is normalized to 1 in the IR limit of vanishing photon energy.

is a forward-backward asymmetry in the photon angular distribution in analogy with the two-body final states [8]. It could be of interest to search for this at the Tevatron⁷.

While the difference between the two cases is rather striking, as displayed by the ratio in Fig. 2, it should be kept in mind that there are singularities along the edges $x_1 = 0.5$ and $x_2 = 0.5$. Thus, when an integrated cross section is considered, these singular parts (which are absent in the ratio shown in Fig. 2) play an important role, and tend to reduce the difference between the graviton- and photon-exchange cases.

8 Discussion

We show in Fig. 3 the integrated, dimensionless cross sections of Eqs. (39) and (40) *vs.* x_3^{\min} , where we have integrated over $x_3^{\min} \leq x_3 \leq 0.5$, subject to y -cuts: $s_1, s_2 \geq y\hat{s}$, $s_3 \geq y_3\hat{s}$. Three values of the y -cut are considered, $y = 0.01, 0.02, 0.05$, whereas y_3 , which controls the minimum invariant mass of the two muons, has been held fixed at 0.01. At a scale $\sqrt{\hat{s}} = 1$ TeV, the most loose cut of $y = 0.01$ corresponds to muon (or photon) energies exceeding 10 GeV. The corresponding angular cuts are well within the resolutions foreseen at the LHC [18].

With the integrated dimensionless cross sections given in Fig. 3, and the convolution integrals given by Eqs. (8) and (36), one may define a “figure of merit” as the ratio of the graviton cross section to the Drell–Yan background. For the ADD scenario, this will take

⁷At the LHC, such asymmetries would be absent, since the two beams are identical.

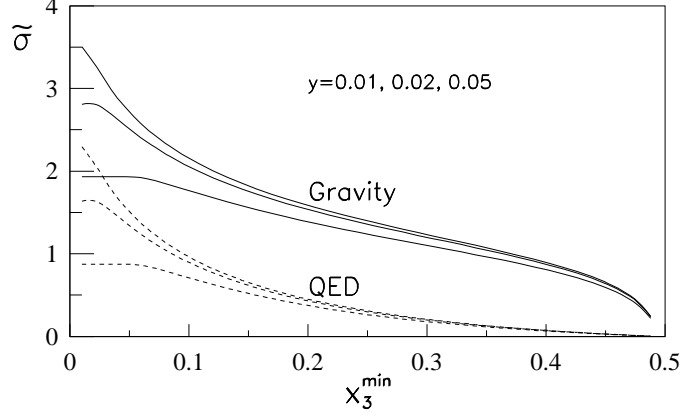


Figure 3: Integrated dimensionless cross sections of Eqs. (39) and (40) vs. x_3^{\min} . Solid: graviton exchange, dashed: QED. Three values of y -cut are considered, as indicated, from top to bottom.

the form

$$R^{\text{ADD}} = \frac{9}{640} \frac{|C_4|^2 \hat{s}^4}{\alpha^2} \frac{I_{gg}(\hat{s})}{I_{q\bar{q}}(\hat{s})} \frac{\tilde{\sigma}_{gg \rightarrow \mu^+ \mu^- \gamma}^{(G)}}{\tilde{\sigma}_{q\bar{q} \rightarrow \mu^+ \mu^- \gamma}^{(\gamma)}}, \quad (41)$$

whereas for the RS scenario (in the narrow-width approximation), the resolution δ_s enters:

$$R^{\text{RS}} = \frac{9}{2048} \frac{(\kappa m_G)^2}{\alpha^2} \frac{1}{\delta_s \gamma_G} \frac{I_{gg}(m_G^2)}{I_{q\bar{q}}(m_G^2)} \frac{\tilde{\sigma}_{gg \rightarrow \mu^+ \mu^- \gamma}^{(G)}}{\tilde{\sigma}_{q\bar{q} \rightarrow \mu^+ \mu^- \gamma}^{(\gamma)}}. \quad (42)$$

In order to estimate the total number of $\mu^+ \mu^- \gamma$ events produced, we consider the sum of QED and graviton-induced cross sections in Figs. 4 and 5. Here, we have chosen a y -cut of 0.01, and consider a minimum x_3 of 0.1⁸.

For the ADD scenario (Fig. 4), we plot $d\sigma/d\sqrt{\hat{s}}$ according to Eqs. (22), (37), (39) and (40) (dashed). These curves are scaled by a factor of 100, and thus give the cross section per 100 GeV bin. Also shown, as solid curves, are the integrated cross sections:

$$\sigma(\sqrt{\hat{s}}) = \int_{\sqrt{\hat{s}}}^{M_S} d\sqrt{\hat{s}'} \frac{d\sigma}{d\sqrt{\hat{s}'}}. \quad (43)$$

The line at 10^{-2} fb corresponds to 1 event per year, at the integrated LHC luminosity of 100 fb^{-1} (one nominal LHC year at $L = 10^{34} \text{ cm}^{-2} \text{ s}^{-1}$). Finally, the dotted curve labelled R shows the “figure-of-merit”, Eq. (41). We consider two values for the number of extra

⁸These cuts have not been optimized.

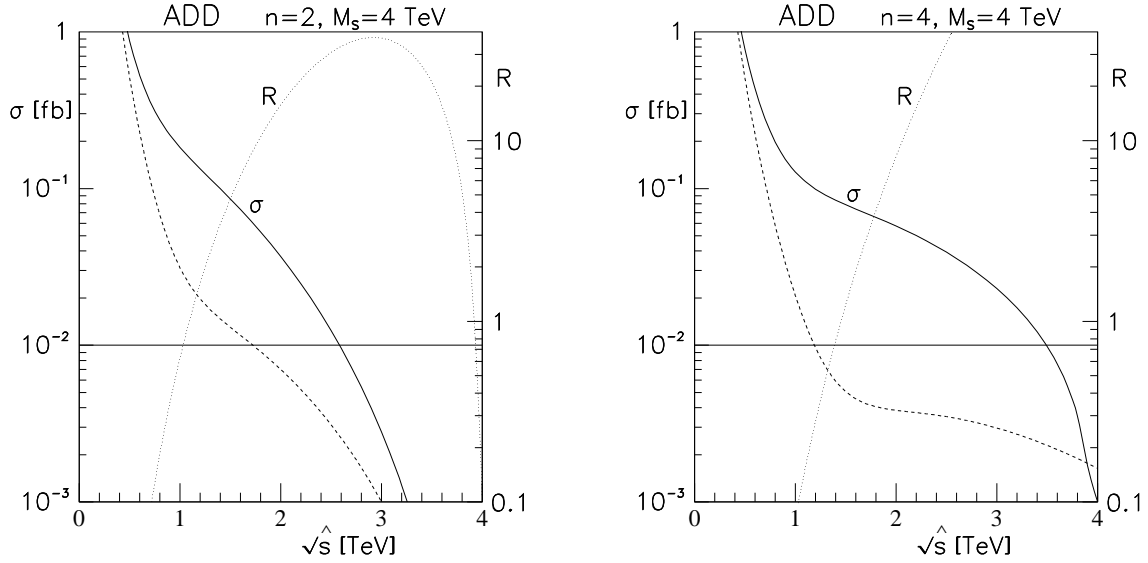


Figure 4: ADD case, $n = 2$ and $n = 4$, $M_S = 4$ TeV. Differential cross section, $100 \times d\sigma/d\sqrt{\hat{s}}$ (dashed) in [fb/GeV], integrated cross section, $\sigma(\sqrt{\hat{s}})$ (solid), Eq. (43), and signal to QED ratio, R (dotted).

dimensions, $n = 2$ and 4 , and take the string scale, M_S , to be 4 TeV. It is seen that there will be a significant number of such Bremsstrahlung events up to a few TeV, and that for the larger values of $\sqrt{\hat{s}}$, these tend to be gravity-dominated.

In the RS case, we consider $k/\overline{M}_{\text{Pl}} = 0.01$ and 0.05 , and a resolution roughly approximated as $\delta_{\hat{s}} = 10\%$. We display the corresponding signal plus QED background cross sections, given by Eqs. (32) and (39) (divided by $\Delta\hat{s}$), together with (35) and (40) (solid). Also shown, is the ratio of gravity-induced to QED cross section, as given by the “figure of merit”, Eq. (42).

In summary, we have discussed Bremsstrahlung induced by the exchange of massive gravitons at hadron colliders, in particular at the LHC. Both the ADD and the RS scenarios have been considered. We found that three-body final states can be a valuable supplement to the two-body final states, for the purpose of detecting massive gravitons related to extra dimensions. These configurations, of a hard photon associated with a muon pair in the opposite direction, should provide a striking signal at the LHC.

We have here focused on gluon fusion. There is also graviton exchange induced by quark-antiquark annihilation. These contributions are of importance at larger invariant masses, and will be discussed elsewhere [15]. It could also be interesting to consider similar processes where the final-state fermions are massive.

Acknowledgements. It is a pleasure to thank Paolo di Vecchia for very useful discussions. This research has been supported by the Research Council of Norway and by NORDITA.

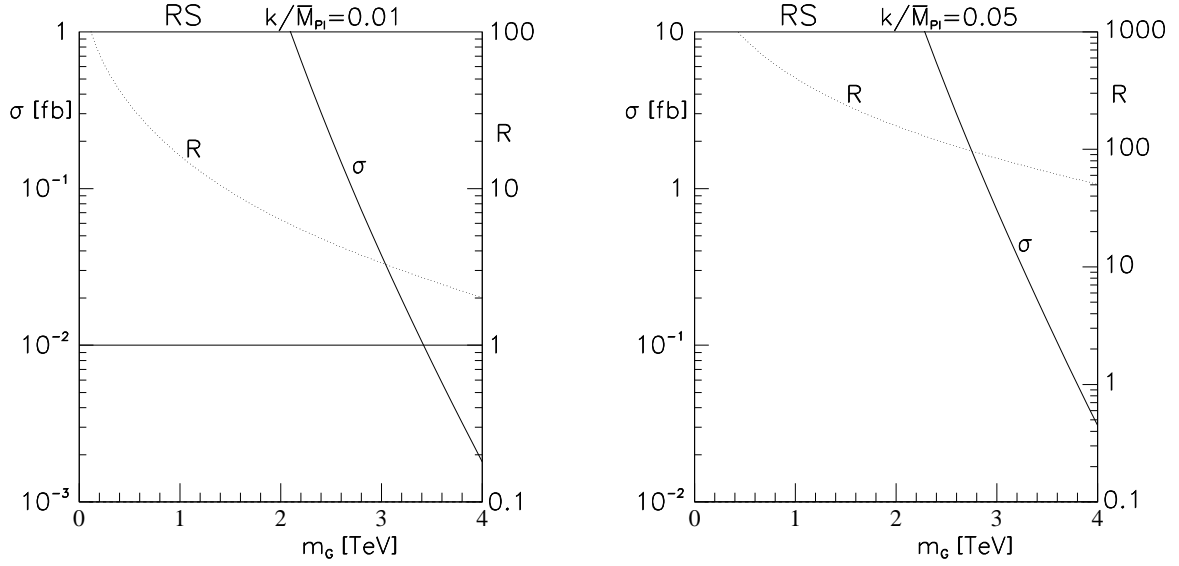


Figure 5: RS case, $k/\overline{M}_{\text{Pl}} = 0.01$ and 0.05 . Cross sections and signal to QED ratio. The graviton-exchange cross section is evaluated in the narrow-width approximation, with the resolution $\delta_{\hat{s}} = 0.10$.

References

- [1] I. Antoniadis, Phys. Lett. B **246** (1990) 377.
- [2] E. Witten, Nucl. Phys. B **443** (1995) 85 [hep-th/9503124];
P. Hořava and E. Witten, Nucl. Phys. B **460** (1996) 506 [hep-th/9510209];
P. Hořava and E. Witten, Nucl. Phys. B **475** (1996) 94 [hep-th/9603142].
- [3] N. Arkani-Hamed, S. Dimopoulos and G. Dvali, Phys. Lett. B **429** (1998) 263 [hep-ph/9803315];
N. Arkani-Hamed, S. Dimopoulos and G. Dvali, Phys. Rev. D **59** (1999) 086004 [hep-ph/9807344].
- [4] L. Randall and R. Sundrum, Phys. Rev. Lett. **83** (1999) 3370 [hep-ph/9905221];
L. Randall and R. Sundrum, Phys. Rev. Lett. **83** (1999) 4690 [hep-th/9906064].
- [5] G. F. Giudice, R. Rattazzi and J. D. Wells, Nucl. Phys. B **544** (1999) 3 [hep-ph/9811291].
- [6] E. A. Mirabelli, M. Perelstein and M. E. Peskin, Phys. Rev. Lett. **82** (1999) 2236 [hep-ph/9811337];
S. Cullen, M. Perelstein and M. E. Peskin, Phys. Rev. D **62** (2000) 055012 [hep-ph/0001166].
- [7] T. Han, J. D. Lykken and R. Zhang, Phys. Rev. D **59** (1999) 105006 [hep-ph/9811350].

- [8] J. L. Hewett, Phys. Rev. Lett. **82** (1999) 4765 [hep-ph/9811356].
- [9] K. Cheung, Phys. Rev. D **61** (2000) 015005 [hep-ph/9904266].
- [10] H. Davoudiasl, J. L. Hewett and T. G. Rizzo, Phys. Rev. Lett. **84** (2000) 2080 [hep-ph/9909255].
- [11] H. Davoudiasl, J. L. Hewett and T. G. Rizzo, Phys. Rev. D **63** (2001) 075004 [hep-ph/0006041].
- [12] J. Bijnens, P. Eerola, M. Maul, A. Månsson and T. Sjöstrand, Phys. Lett. B **503** (2001) 341 [hep-ph/0101316].
- [13] G. Landsberg, hep-ex/0009038.
- [14] S. Hannestad and G. Raffelt, hep-ph/0103201.
- [15] E. Dvergsnes, P. Osland and N. Öztürk, to be published.
- [16] H. A. Olsen, P. Osland and I. Øverbø, Nucl. Phys. B **171** (1980) 209.
- [17] B. C. Allanach, K. Odagiri, M. A. Parker and B. R. Webber, JHEP **0009** (2000) 019 [hep-ph/0006114].
- [18] See e.g., *ATLAS detector and Physical Performance Technical Design Report*, <http://atlasinfo.cern.ch/Atlas/GROUPS/PHYSICS/TDR/access.html>, G. L. Bayatian *et al.*, *CMS Technical Proposal*, CERN LHCC 94-38 (1994), <http://cmsinfo.cern.ch/TP/TP.html>.